Inorganic Chemistry
Article

Inorg. Chem. **2009**, *48*, 9377–9384 **9377**
DOI: 10.1021/ic901175e

Toward Unidirectional Rotary Motion in Nickelacarboranes: Characterization of Diastereomeric Nickel Bis(Dicarbollide) Complexes Derived from the [*Nido*-7-CH_3-7,8-$C_2B_9H_{11}$]$^-$ Anion

Robert D. Kennedy, Carolyn B. Knobler, and M. Frederick Hawthorne*,†

Department of Chemistry and Biochemistry, University of California at Los Angeles, 607 Charles E. Young Drive (East), Los Angeles, California 90095. †International Institute of Nano and Molecular Medicine, 1514 Research Park Drive, University of Missouri, Columbia, MO 65211.

Received June 22, 2009

Two diastereomeric pairs of nickel bis(*C*-monomethyldicarbollide) complexes, derived from the racemic [*nido*-7-CH_3-7,8-$C_2B_9H_{11}$]$^-$ anion, have been synthesized and characterized by NMR spectroscopy and single-crystal X-ray diffraction analysis. Neutral (*dd/ll*) [1(2),1′(2′)-Me_2-*closo*-3,1,2-$Ni^{IV}C_2B_9H_{10}$-{3:3′}-*closo*-3′,1′,2′-$Ni^{IV}C_2B_9H_{10}$] **1** and (*meso*) [1,2′-Me_2-*closo*-3,1,2-$Ni^{IV}C_2B_9H_{10}$-{3:3′}-*closo*-3′,1′,2′-$Ni^{IV}C_2B_9H_{10}$] **2** adopt typical *cisoid* conformations in the solid state. The temperature-dependent ^{11}B and ^{1}H NMR spectra of **2** indicate that the energy barrier to the interconversion of racemic rotational isomers is 66.5 ± 2 kJ/mol. In the solid state, the $[NMe_4]^+$ salts of the (*dd/ll*) [1(2),1′(2′)-Me_2-*closo*-3,1,2-$Ni^{III}C_2B_9H_{10}$-{3:3′}-*closo*-3′,1′,2′-$Ni^{III}C_2B_9H_{10}$]$^-$ anion **NMe_4·3** and the (*meso*) [1,2′-Me_2-*closo*-3,1,2-$Ni^{III}C_2B_9H_{10}$-{3:3′}-*closo*-3′,1′,2′-$Ni^{III}C_2B_9H_{10}$]$^-$ anion **NMe_4·4** adopt *gauche* and *transoid* configurations, respectively, with *transoid* methyl substituents in both cases.

Introduction

The incorporation of unidirectional rotary motion into molecular machines is a stimulating challenge of nanotechnology. So far, the systems investigated successfully by many groups have been diverse in terms of complexity, stimuli, and the type of motion produced. Extensive reviews of artificial molecular rotors have appeared recently.[1] For rotation to do useful work it must be unidirectional, and unidirectional rotation is a chiral phenomenon, thus requiring chirality to be built usefully into the system. Feringa et al. have designed several elegant molecular rotors in which unidirectional rotation occurs through successive photoinduced alkene *cis-trans* isomerizations and thermal relaxations.[2] Kelly et al. have developed a triptycene-helicene system where unidirectional rotation is driven by chemical energy and thermal relaxation.[3] A combination of light energy and chemical energy is used to drive the unidirectional rotation in Leigh's catenane systems.[4]

Hawthorne et al. recently reinvestigated the redox- or photocontrolled rotary motion displayed by the nickel bis(dicarbollide) sandwich complex, [*closo*-3,1,2-$NiC_2B_9H_{11}$-{3:3′}-*closo*-3′,1′,2′-$NiC_2B_9H_{11}$].[5] This compound was first reported in 1967.[6] They proposed that redox or photoexcitation of the metallacarborane causes a rotation of the dicarbollide ligands with respect to each other. The ligands of this neutral Ni^{IV} complex are arranged in such a way that the cage carbons are in a staggered *cisoid* configuration on the same side of the molecule, evidenced by the strong dipole moment of 6.16 D in cyclohexane solution, and by the results of a single-crystal X-ray diffraction analysis.[7] Computational work has shown that, in the case of the Ni^{IV} species, there is a global minimum corresponding to the staggered *cisoid* configuration,[5,8] and it has been suggested that this rotamer is

*To whom correspondence should be addressed. E-mail: hawthornem@missouri.edu.

(1) (a) Kottas, G. S.; Clarke, L. I.; Horinek, D.; Michl, J. *Chem. Rev.* **2005**, *105*, 1281–1376. (b) Browne, W. R.; Feringa, B. L. *Nat. Nanotechnol.* **2006**, *1*, 25–35. (c) Kay, E. R.; Leigh, D. A.; Zerbetto, F. *Angew. Chem., Int. Ed.* **2007**, *46*, 72–191. (d) Mandl, C. P.; König, B. *Angew. Chem., Int. Ed.* **2004**, *43*, 1622–1624.

(2) (a) ter Wiel, M. K. J.; van Delden, R. A.; Meetsma, A.; Feringa, B. L. *J. Am. Chem. Soc.* **2003**, *125*, 15076–15086. (b) Vicario, J.; Walko, M.; Meetsma, A.; Feringa, B. L. *J. Am. Chem. Soc.* **2006**, *128*, 5127–5135.

(3) Kelly, T. R.; Cai, X.; Damkaci, F.; Panicker, S. B.; Tu, B.; Bushell, S. M.; Cornella, I.; Piggott, M. J.; Salives, R.; Cavero, M.; Zhao, Y.; Jasmin, S. *J. Am. Chem. Soc.* **2007**, *129*, 376–386.

(4) Leigh, D. A.; Wong, J. K. Y.; Dehez, F.; Zerbetto, F. *Nature* **2003**, *424*, 174.

(5) (a) Hawthorne, M. F.; Zink, J. I.; Skelton, J. M.; Bayer, M. J.; Liu, C.; Livshits, E.; Baer, R.; Neuhauser, D. *Science* **2004**, *303*, 1849–1851. (b) Hawthorne, M. F.; Ramachandran, B. M.; Kennedy, R. D.; Knobler, C. B. *Pure Appl. Chem.* **2006**, *78*, 1299–1304.

(6) (a) Warren, L. F., Jr.; Hawthorne, M. F. *J. Am. Chem. Soc.* **1967**, *89*, 470–471. (b) Hawthorne, M. F.; Young, D. C.; Andrews, T. D.; Howe, D. V.; Pilling, R. L.; Pitts, A. D.; Reintjes, M.; Warren, L. F., Jr.; Wegner, P. A. *J. Am. Chem. Soc.* **1968**, *90*, 879–896.

(7) St. Clair, D.; Zalkin, A.; Templeton, D. H. *J. Am. Chem. Soc.* **1970**, *92*, 1173–1179.

(8) Bühl, M.; Holub, J.; Hnyk, D.; Macháček, J. *Organometallics* **2006**, *25*, 2173–2181.

Published on Web 09/11/2009

stabilized because of favorable bonding overlap between molecular orbitals on the two opposing ligands. In solution at ambient temperature, ^{1}H, ^{11}B, and ^{13}C NMR spectroscopy indicates that the cages of the Ni^{IV} bis(dicarbollide) are not locked in a static *cisoid* conformation, but it is not known if they are rocking back and forth between the two *cisoid* isomers through an eclipsed *cisoid* intermediate, or if rotation occurs through a *transoid* conformation. However, the calculated barriers for these two processes are similar, and low (27.7 kJ/mol) and full rotation is expected at room temperature.[5,8]

In the solid state, the cage carbon atoms in the unsubstituted Ni^{III} bis(dicarbollide) anion are in a *transoid* orientation, and this has been attributed to the strong intramolecular dipole−dipole interaction between the ligands.[9] No stabilizing orbital overlap occurs at any particular angle because, in contrast to the Ni^{IV} bis(dicarbollide) complex, the highest occupied molecular orbital (HOMO) is localized on the metal center and within each cage. Although the global minimum corresponds to the staggered *transoid* orientation, the barriers to rotation in the Ni^{III} species are somewhat lower than in the Ni^{IV} species, which may account for the variety of conformations observed in the crystal structures of Ni^{III} bis(dicarbollide) complexes.[10]

Although the rotation in the unsubstituted nickel bis(dicarbollide) system is neither unidirectional nor continuous, further investigation was deemed desirable for a number of reasons:

(a) It was noted that substitution at the cage carbon atoms could provide the chirality necessary for unidirectional rotary motion[5] (Figure 1).

(b) The rotation created by the system may be harnessed and incorporated into a device via the rich and varied substitution chemistry of *ortho*-carborane and metal bis(dicarbollide) complexes.[10,11]

(c) Although metal bis(dicarbollide) complexes are notoriously chemically robust, it is not known how the nature and position of functionality may affect the rotary motion.

(d) Definitive experimental evidence of a barrier to rotation in a Ni^{IV} species is required, as this is an essential property of a functioning rotor. Variable-temperature NMR spectroscopy has been used successfully to probe rotational energy barriers in a number of metal dicarbollide systems,[12,13] and calculations at various levels of theory reproduce the experimental results satisfactorily.[5,8,12,13]

(e) Chirality in boranes and carborane clusters is an area requiring extensive investigation,[14] and there are few crystal structures of diastereomeric metal bis(dicarbollide) complexes.[15−17] Also, the majority of crystallographically characterized chiral metal bis(dicarbollide) complexes are d^6 Co^{III} derivatives, often locked in a particular conformation through an *exo* ligand−ligand bridge.[10] The large majority of Ni^{III} derivatives characterized by single-crystal X-ray diffraction analysis have no cage substitution, and the parent anion is usually crystallized with an unusual cation. Charge-transfer complexes have dominated the crystallographic characterization of Ni^{IV} compounds.[11]

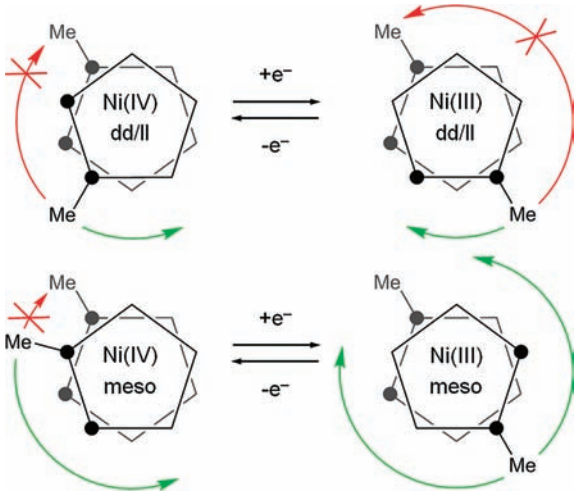

Figure 1. Basis for redox-controlled unidirectional rotation in a bis(dicarbollide) nickel complex. C_2B_3 bonding faces are represented by pentagons. Filled circles represent C−H or C−Me vertices, unmarked vertices represent B−H vertices.

Here we report the solid-state structures and the results of "dynamic" NMR spectroscopy from a diastereomeric nickel bis(*C*-monomethyldicarbollide) system.

Experimental Section

General Considerations. A mixture of (*dd*/*ll*) [1(2),1′(2′)-Me_2-*closo*-3,1,2-$Ni^{IV}C_2B_9H_{10}$-{3:3′}-*closo*-3′,1′,2′-$Ni^{IV}C_2B_9H_{10}$] **1** and (*meso*) [1,2′-Me_2-*closo*-3,1,2-$Ni^{IV}C_2B_9H_{10}$-{3:3′}-*closo*-3′,1′,2′-$Ni^{IV}C_2B_9H_{10}$] **2** (1:1 mixture of diastereomers, determined by ^{1}H NMR in dichloromethane-d_2) was prepared as described previously.[18,20,21] All reagents were reagent-grade and used as

(9) Hansen, F. V.; Hazell, R. G.; Hyatt, C.; Stucky, G. D. *Acta Chem. Scand.* **1973**, *27*, 1210–1218.
(10) (a) Corsini, M.; de Biani, F. F.; Zanello, P. *Coord. Chem. Rev.* **2006**, *250*, 1351–1372. (b) Bregadze, V. I. *Chem. Rev.* **1992**, *92*, 209–223. (c) Sivaev, I. B.; Bregadze, V. I. *Collect. Czech. Chem. Commun.* **1994**, *64*, 783–805.
(11) (a) Sivaev, I. B.; Bregadze, V. I. *J. Organomet. Chem.* **2000**, *614*−*615*, 27–36. (b) Schubert, D. M.; Harwell, D. E.; Knobler, C. B.; Hawthorne, M. F. *Acta Chem. Scand.* **1999**, *53*, 721–730.
(12) Núñez, R.; Tutusaus, O.; Teixidor, F.; Viñas, C.; Sillanpää, R.; Kivekäs, R. *Chem.—Eur. J.* **2005**, *11*, 5637–5647.
(13) (a) Viñas, C.; Llop, J.; Teixidor, F.; Kivekäs, R.; Sillanpää, R. *Chem.—Eur. J.* **2005**, *11*, 1933–1941. (b) O'Connell, D.; Patterson, J. C.; Spalding, T. R.; Ferguson, G.; Gallagher, J. F.; Li, Y.; Kennedy, J. D.; Macías, R.; Thornton-Pett, M.; Holub, J. *J. Chem. Soc., Dalton Trans.* **1996**, 3323–3333. (c) Marder, T. B.; Baker, R. T.; Long, J. A.; Doi, J. A.; Hawthorne, M. F. *J. Am. Chem. Soc.* **1981**, *103*, 2988–2994.
(14) Plešek, J. *Inorg. Chim. Acta* **1999**, *289*, 45–50.
(15) Corsini, M.; Zanello, P.; Kudinov, A. R.; Meshcheryakov, V. I.; Perekalin, D. S.; Lyssenko, K. A. *J. Solid State Electrochem.* **2005**, *9*, 750–757.
(16) (a) Yan, Y.-K.; Mingos, D. M. P.; Müller, T. E.; Williams, D. J.; Kurmoo, M. *J. Chem. Soc., Dalton Trans.* **1994**, 1735–1741. (b) Yan, Y.-K.; Mingos, D. M. P.; Williams, D. J. *J. Organomet. Chem.* **1995**, *498*, 267–274.
(17) Viñas, C.; Bertran, J.; Gomez, S.; Teixidor, F.; Dozol, J.-F.; Rouquette, H.; Kivekäs, R.; Sillanpää, R. *J. Chem. Soc., Dalton Trans.* **1998**, 2849–2854.
(18) Warren, L. F., Jr.; Hawthorne, M. F. *J. Am. Chem. Soc.* **1970**, *92*, 1157–1173.
(19) Chamberlain, R. M.; Scott, B. L.; Melo, M. M.; Abney, K. D. *Inorg. Chem.* **1997**, *36*, 809–817.
(20) Hawthorne, M. F.; Andrews, T. D.; Garrett, P. M.; Olsen, F. P.; Reintjes, M.; Tebbe, F. N.; Warren, L. F.; Wegner, P. A.; Young, D. C.; Alexander, R. P.; Blundon, R. W.; Schroeder, H. A.; Heying, T. L. *Inorg. Synth* **1967**, *10*, 91–118.
(21) Hawthorne, M. F.; Young, D. C.; Garrett, P. M.; Owen, D. A.; Schwerin, S. G.; Tebbe, F. N.; Wegner, P. A. *J. Am. Chem. Soc.* **1968**, *90*, 862–868.

purchased. ^{1}H, ^{11}B, ^{13}C NMR spectra were measured on Bruker ARX 400, ARX 500, and DRX 500 spectrometers. Chemical shift values for ^{1}H NMR and ^{13}C-{^{1}H} NMR were referenced relative to solvent resonances. Chemical shift values for ^{11}B NMR were referenced relative to external $BF_3 \cdot OEt_2$. Complex multiplets are denoted with "m".

Separation of (*dd*/*ll*) [1(2),1′(2′)-Me$_2$-*closo*-3,1,2-Ni^{IV}C$_2$B$_9$H$_{10}$-{3:3′}-*closo*-3′,1′,2′-Ni^{IV}C$_2$B$_9$H$_{10}$], 1 and (*meso*) [1,2′-Me$_2$-*closo*-3,1,2-Ni^{IV}C$_2$B$_9$H$_{10}$-{3:3′}-*closo*-3′,1′,2′-Ni^{IV}C$_2$B$_9$H$_{10}$], 2. A 1:1 mixture of compounds **1** and **2** (500 mg, 1.42 mmol) was partially dissolved in a small volume (2 mL) of dichloromethane at room temperature and shaken. The solid was removed by filtration and dissolved in a minimum of dichloromethane (5 mL). Upon cooling to −18 °C, pure compound **1** precipitated as a bright orange powder that was isolated by filtration (142 mg, 0.404 mmol, 28%). Crystals of compound **1** suitable for single-crystal X-ray diffraction analysis were grown by slow evaporation from a saturated solution in benzene-heptane. The combined mother liquors were concentrated and cooled to −18 °C. The resulting orange precipitate was removed by filtration, and the filtrate was concentrated and cooled to −18 °C. The deep red supernatant liquid was decanted leaving compound **2** as red-orange crystals (30 mg, 0.085 mmol, 6%). Crystals of compound **2** suitable for single-crystal X-ray diffraction analysis were grown by slow evaporation from a saturated solution in dichloromethane-heptane. Data for compound **1**: ^{1}H NMR (299 K, 400 MHz, CD_2Cl_2) δ 2.46 (s, 6H, CH_3); 4.05 (br, s, 2H, $C_{cage}-H$). ^{13}C{^{1}H} NMR (299 K, 100 MHz, CD_2Cl_2) δ 31.94 (*C*H$_3$); 76.44; 86.73. ^{11}B NMR (299 K, 160 MHz, CD_2Cl_2) δ −10.5 (d, 1B, $^{1}J_{BH}$ = 171 Hz); −5.6 (d, 1B, $^{1}J_{BH}$ = 165 Hz); −0.9 (d, 2B, $^{1}J_{BH}$ = 156 Hz); 3.8 (d, 1B, $^{1}J_{BH}$ = 172 Hz); 5.7 (d, 2B, $^{1}J_{BH}$ = 151 Hz); 16.4 (d, 1B, $^{1}J_{BH}$ = 145 Hz); 22.5 (d, 1B, $^{1}J_{BH}$ = 158 Hz). Data for **2**: ^{1}H NMR (299 K, 400 MHz, $CDCl_3$) δ 2.47 (s, 6H, CH_3); 4.48 (br, s, 1H, $C_{cage}-H$); 4.00 (br, s, 1H, $C_{cage}-H$), (299 K, 400 MHz, toluene-d_8) δ 1.42 (s, 3H, CH_3); 1.74 (s, 3H, CH_3); 3.06 (br, s, 1H, $C_{cage}-H$); 3.32 (br, s, 1H, $C_{cage}-H$), (370 K, 400 MHz, toluene-d_8) δ 1.82 (s, 6H, CH_3); 3.50 (s, 2H, $C_{cage}-H$). ^{13}C{^{1}H} NMR (300 K, 100 MHz, $CDCl_3$) δ 29.79, 31.07, 69.77, 72.77. ^{11}B NMR (299 K, 160 MHz, toluene-d_8) δ −10.7 (1B); −9.9 (1B); −6.7 (d, 2B, $^{1}J_{BH}$ = 156 Hz); −2.8 (d, 1B, $^{1}J_{BH}$ = 160 Hz); 0.0 (m, 4B); 1.4 (m, 2B); 2.9 (1B); 4.7 (d, 1B, $^{1}J_{BH}$ = 153 Hz); 5.6 (d, 1B, $^{1}J_{BH}$ = 151 Hz); 7.4 (d, 1B, $^{1}J_{BH}$ = 158 Hz); 16.0 (1B); 16.5 (1B); 20.3 (d, 2B, $^{1}J_{BH}$ = 134 Hz), (371 K, 160 MHz, toluene-d_8) δ −9.5 (d, 2B, $^{1}J_{BH}$ = 175 Hz); −5.9 (d, 2B, $^{1}J_{BH}$ = 167 Hz); −0.5 (d, 2B, $^{1}J_{BH}$ = 144 Hz); 2.1 (2B); 3.0 (2B); 4.3 (2B); 5.8 (2B); 16.9 (d, 2B, $^{1}J_{BH}$ = 148 Hz); 21.4 (d, 2B, $^{1}J_{BH}$ = 158).

Preparation of (*dd*/*ll*) NMe$_4$[1(2),1′(2′)-Me$_2$-*closo*-3,1,2-Ni^{III}C$_2$B$_9$H$_{10}$-{3:3′}-*closo*-3′,1′,2′-Ni^{III}C$_2$B$_9$H$_{10}$], NMe$_4$·3. The following reaction was conducted in air. Excess anhydrous sodium borohydride (0.5 g) was added to compound **1** (160 mg 0.455 mmol) in methanol (10 mL). Effervescence occurred, and the solution became dark brown. After stirring for 30 min, water was added (20 mL), and the methanol was removed under reduced pressure. Excess [NMe$_4$]Br (0.5 g) was added. The fine brown precipitate was isolated by filtration, washed with water, and dried under vacuum. A portion of the brown solid was dissolved in acetonitrile and filtered, and a small volume of water was added to the filtrate. Crystals of compound **NMe$_4$·3** suitable for single-crystal X-ray diffraction analysis were grown by allowing the filtrate to evaporate slowly at room temperature. The paramagnetic nature of the Ni^{III} center prevented useful NMR data from being obtained. Mp: > 250 °C.

Similarly, the [NHMe$_3$]$^{+}$, *N*-methylpyridinium, [PPh$_4$]$^{+}$, [NEt$_4$]$^{+}$, [N(*n*-Bu)$_4$]$^{+}$ and Cs^{+} salts were prepared by treating the aqueous solution of (*dd*/*ll*) Na[1(2),1′(2′)-Me$_2$-*closo*-3,1,2-Ni^{III}C$_2$B$_9$H$_{10}$-{3:3′}-*closo*-3′,1′,2′-Ni^{III}C$_2$B$_9$H$_{10}$] with [NHMe$_3$]-Cl, *N*-methylpyridinium iodide, [PPh$_4$]Br, [NEt$_4$]Br, [N(*n*-Bu)$_4$]Br, and CsCl, respectively. Crystals of compound **MeNC$_5$H$_5$·3** suitable for single-crystal X-ray diffraction analysis were grown by slow evaporation of a methanol solution at room temperature.

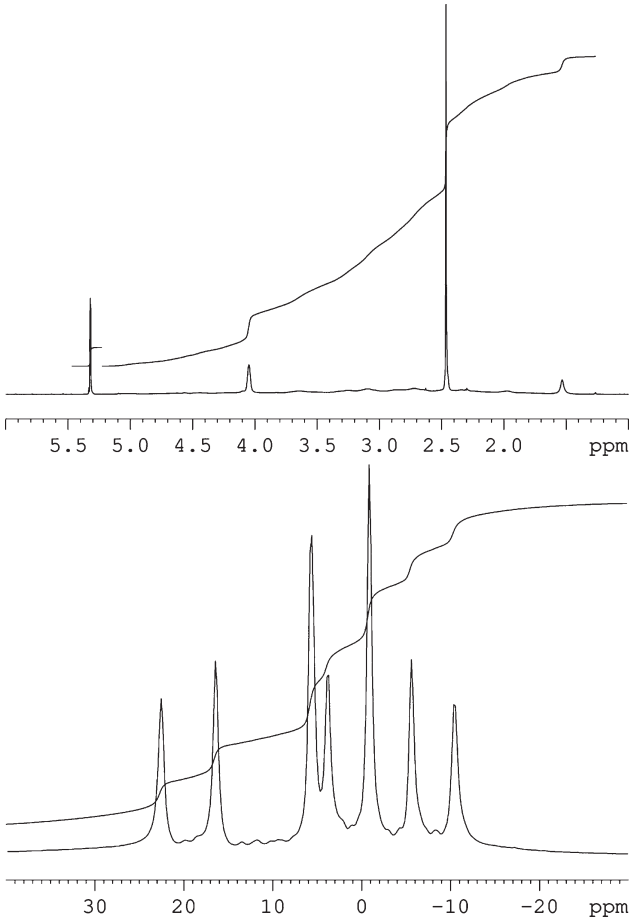

Figure 2. ^{1}H (top) and ^{11}B-{^{1}H} (bottom) NMR spectra of compound **1**, recorded in CD_2Cl_2. The residual solvent signal appears at 5.32 ppm in ^{1}H NMR spectrum.

Scheme 1. Synthesis of Compounds **1** and **2**[a]

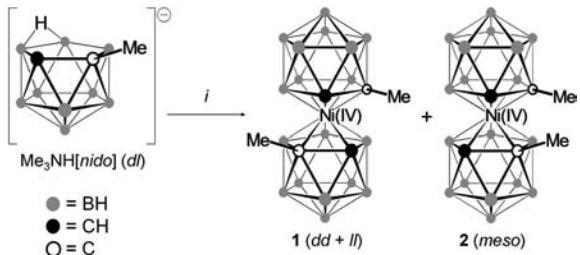

[a] Reagents: (i) NaH (2 equiv), THF, reflux; Ni(acac)$_2$, THF, 25 °C; air, THF; CsCl, H_2O; $FeCl_3$, H_2O.

Preparation of (*meso*) [NMe$_4$][1,2′-Me$_2$-*closo*-3,1,2-Ni^{III}C$_2$B$_9$H$_{10}$-{3:3′}-*closo*-3′,1′,2′-Ni^{III}C$_2$B$_9$H$_{10}$], NMe$_4$·4. Compound **4** was prepared from a solution of compound **2** (100 mg) in methanol (10 mL) in an identical fashion to the preparation of compound **3**. Slow evaporation of a filtered solution of compound **NMe$_4$·4** in acetonitrile-water resulted in crystals suitable for X-ray diffraction analysis. The paramagnetic nature of the Ni^{III} center prevented useful NMR data from being obtained. Mp: > 250 °C.

Preparation of [NMe$_4$][*closo*-3,1,2-Ni^{III}C$_2$B$_9$H$_{11}$-{3:3′}-*closo*-3′,1′,2′-Ni^{III}C$_2$B$_9$H$_{11}$]. This compound was prepared as described previously. Crystals suitable for single-crystal X-ray diffraction analysis were grown by slow evaporation of a methanol solution at room temperature.

Table 1. Single Crystal X-ray Diffraction Data Collection and Structure Parameters for **1**, **2**, $NMe_4 \cdot 3$, $MeNC_5H_5 \cdot 3$, $NMe_4 \cdot 4$, and $NMe_4[Ni^{III}(C_2B_9H_{11})_2]$

	compound					
	1	**2**	$NMe_4 \cdot 3$	$MeNC_5H_5 \cdot 3$	$NMe_4 \cdot 4$	$NMe_4[Ni^{III}(C_2B_9H_{11})_2]$
empirical formula	$C_6H_{26}B_{18}Ni$	$C_6H_{26}B_{18}Ni$	$C_{10}H_{38}B_{18}NNi$	$C_{12}H_{34}B_{18}NNi$	$C_{10}H_{38}B_{18}NNi$	$C_8H_{34}B_{18}NNi$
formula weight	351.56	351.56	425.70	445.69	425.70	397.66
crystal description	orange parallelepiped	orange plate	orange-brown needle	orange-brown plate	red parallele-piped	red needle
crystal size (mm)	0.50 × 0.50 × 0.50	0.50 × 0.35 × 0.10	0.50 × 0.10 × 0.075	0.4 × 0.1 × 0.05	0.25 × 0.25 × 0.20	0.30 × 0.25 × 0.20
crystal system	orthorhombic	monoclinic	monoclinic	monoclinic	monoclinic	orthorhombic
space group	*Pbca*	*Cc*	*C*2/*c*	*C*2/*c*	*C*2/*c*	*Cmcm*
temperature (K)	100(2)	298(2)	298(2)	298(2)	298(2)	298(2)
radiation (λ)	Mo Ka	Mo Ka	Mo Ka	Mo Ka	Mo Ka	Mo Ka
wavelength (Å)	0.71073	0.71073	0.71073	0.71073	0.71073	0.71073
a (Å)	13.2839(12)	13.8137(9)	18.7102(14)	21.2467(13)	10.0649(11)	9.8187(7)
b (Å)	13.4258(12)	8.0692(5)	12.0994(8)	12.4990(8)	10.8581(12)	10.3706(7)
c (Å)	19.9942(18)	16.9295(11)	12.7656(9)	8.8655(6)	22.268(2)	21.8015(15)
α (deg)	90.00	90.00	90.00	90.00	90.00	90.00
β (deg)	90.00	101.3760(10)	124.8140(10)	93.7860(10)	101.996(2)	90.00
γ (deg)	90.00	90.00	90.00	90.00	90.00	90.00
V (Å^3)	3565.9(6)	1850.0(2)	2372.6(3)	2349.2(3)	2380.4(5)	2220.0(3)
Z	8	4	4	4	4	4
d_{calc} (g/cm^3)	1.310	1.262	1.192	1.260	1.188	1.232
absorption coefficient (mm^{-1})	1.071	1.032	0.817	0.829	0.815	0.871
F(000)	1440	720	892	924	892	860
θ_{min}, θ_{max} (deg)	2.04, 28.30	2.45, 28.29	2.14, 28.26	1.89, 28.33	1.87, 28.30	1.87, 28.27
index ranges	$-17 \le h \le 17$, $-16 \le k \le 17$, $-10 \le l \le 26$	$-18 \le h \le 18$, $-10 \le k \le 10$, $-21 \le l \le 22$	$-24 \le h \le 24$ $-16 \le k \le 15$, $-16 \le l \le 16$	$-28 \le h \le 28$ $-16 \le k \le 16$ $-11 \le l \le 11$	$-13 \le h \le 13$ $-14 \le k \le 14$, $-29 \le l \le 29$	$-12 \le$ h 9 $-13 \le 13$ $-27 \le 28$
reflections collected	21032	8010	10552	10406	10143	6842
independent reflections	4368 [R(int) = 0.0271]	4231 [R(int) = 0.0190]	2888 [R(int) = 0.0829]	2856 [R(int) = 0.0752]	2864 [R(int) = 0.0268]	1470 [R(int) = 0.0551]
observed reflections	3921 [$I > 2\sigma(I)$]	3948 [$I > 2\sigma(I)$]	2258 [$I > 2\sigma(I)$]	2379 [$I > 2\sigma(I)$]	2173 [$I > 2\sigma(I)$]	1227 [$I > 2\sigma(I)$]
absorption correction	multiscan	multiscan	none	none	multiscan	none
max. and min transmission	0.920, 1	0.839, 1	0.761, 1	0.741, 1	0.819, 1	
refinement method	full	full	full	full	full	full
data/restraints/ parameters	4368/0/288	4231/2/248	2888/0/171	2856/0/160	2864/0/179	1470/0/95
goodness-of-fit on F^2	0.920	1.109	0.708	0.901	1.054	0.923
final R indices [$I > 2\sigma(I)$]	R_1 = 0.0215	R_1 = 0.0249	R_1 = 0.0380	R_1 = 0.0381	R_1 = 0.0373	R_1 = 0.0290
	wR_2 = 0.0597	wR_2 = 0.0660	wR_2 = 0.1083	wR_2 = 0.0999	wR_2 = 0.0914	wR_2 = 0.0837
R indices (all data)	R_1 = 0.0251	R_1 = 0.0273	R_1 = 0.0515	R_1 = 0.0467	R_1 = 0.0542	R_1 = 0.0350
	wR_2 = 0.0622	wR_2 = 0.0671	wR_2 = 0.1185	wR_2 = 0.1036	wR_2 = 0.1015	wR_2 = 0.0872
Δ (e Å^{-3})	0.300, −0.208	0.404, −0.229	0.501, −0.238	0.456, −0.239	0.447, −0.197	0.398, −0.301

X-ray Crystallography. All data were collected on a Brüker SMART CCD diffractometer. Atoms were located by use of statistical methods. All data were corrected for Lorentz and polarization effects. Data for compounds **1**, **2**, and $NMe_4 \cdot 4$ were corrected for absorption but not for extinction, and the data for compound $NMe_4 \cdot 3$, $MeNC_5H_5 \cdot 3$, and [NMe_4][*closo*-3,1,2-$Ni^{III}C_2B_9H_{11}$-{3:3′}-*closo*-3′,1′,2′-$Ni^{III}C_2B_9H_{11}$] were not corrected for absorption or extinction. For compounds **1**, $NMe_4 \cdot 3$, and $NMe_4 \cdot 4$, the methyl hydrogen atoms were placed in calculated positions, and the positional parameters of all other hydrogen atoms were allowed to vary. All hydrogen atoms were placed in calculated positions for compound **2** and $MeNC_5H_5 \cdot 3$. In all cases, all non-hydrogen atoms were included with anisotropic displacement parameters, and isotropic displacement parameters for hydrogen atoms were based on the values for the attached atoms.

Results and Discussion

The nickel bis(*C*-monomethyldicarbollide) system, derived from the racemic [*nido*-7(8)-Me-7,8-$C_2B_9H_{12}]^-$ anion, was chosen as a model system because of its facile synthesis, robustness, and ready crystallizability. Following the previously described synthesis,[18] (*dd*/*ll*) [1(2),1′(2′)-Me_2-*closo*-3,1,2-$Ni^{IV}C_2B_9H_{10}$-{3:3′}-*closo*-3′,1′,2′-$Ni^{IV}C_2B_9H_{10}$] **1** and (*meso*) [1,2′-Me_2-*closo*-3,1,2-$Ni^{IV}C_2B_9$-{3:3′}-*closo*-3′,1′,2′-$Ni^{IV}C_2B_9H_{10}$] **2** were produced as a 1:1 mixture of diastereomers (Scheme 1).

We now report the separation of the diastereomers by use of repeated low-temperature recrystallizations from dichloromethane.

Structure of (*dd*/*ll*) [1(2),1′(2′)-Me_2-*closo*-3,1,2-$Ni^{IV}C_2B_9H_{10}$-{3:3′}-*closo*-3′,1′,2′-$Ni^{IV}C_2B_9H_{10}$] (1). The less soluble isomer was determined to be the *dd*/*ll* diastereomer **1** for the following reasons: The two ligands are equivalent because of a C_2 symmetry axis which persists as the ligands rotate with respect to each other, resulting in simple ^{11}B, ^1H, and ^{13}C NMR spectra (Figure 2). In addition to the broad multiplets arising from B−H protons, only two resonance positions are present in the 500 MHz ^1H NMR spectrum (measured in dichloromethane-d_2) with a 3:1 ratio of integrals, corresponding to the equivalent methyl groups and the equivalent cage C−H hydrogen atoms, respectively. Correspondingly,

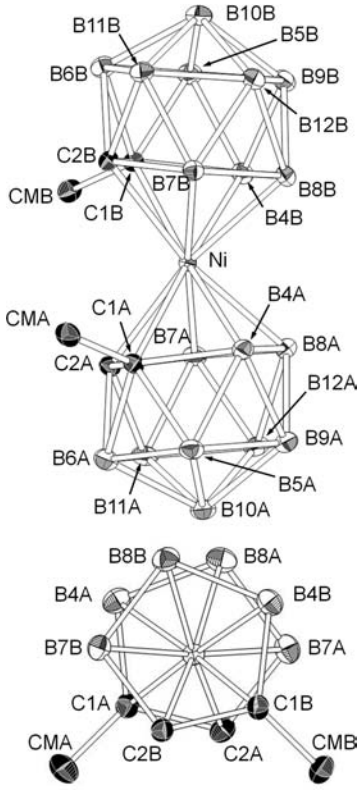

Figure 3. ORTEP representation of a single enantiomer of compound **1** with numbering scheme. Thermal ellipsoids are drawn at 50% probability, and hydrogen atoms are removed for clarity.

seven resonance positions are observed in the 160 MHz ^{11}B NMR spectrum, with a ratio of integrals of 1:2:1:2:1:1:1, those of relative intensity 2 arising from the accidental near-coincidence of signals from chemically inequivalent positions. Single-crystal X-ray diffraction analysis confirmed this isomer to be the *dd*/*ll* diastereomer.

The following notation is used in the description of the structures presented in this paper. In the cases where the two cages are unique, they are designated *A* and *B*. F*A* and F*B* represent the least-squares planes passing thorough the 5 cage atoms of the bonding faces of cages *A* and *B*, respectively. *cent*(F*A*) and *cent*(F*B*) denote the centroids of the bonding faces (C1, C2, B4, B7, B8) of cages *A* and *B*, respectively. Details of the crystal data collection parameters for all compounds are shown in Table 1.

The structure of compound **1** is represented in Figure 3. Selected interatomic distances and angles of all crystallographically characterized compounds are presented in Table 2. Compound **1** crystallizes in the orthorhombic space group *Pbca*. As is typical in Ni^{IV} bis(dicarbollide) complexes, the ligands are in a staggered *cisoid* conformation. The torsion angle described by B8*A*−*cent*(F*A*)−*cent*(F*B*)−B8*B* is 32.26(8)°, deviating slightly from an ideal staggered *cisoid* angle of 36°. In this context it is worthwhile to note that the bonding faces are irregular pentagons. The methyl substituents are in a "*gauche*" conformation, situated on the "outer" cage carbon atoms. There are no significant intramolecular interactions. Each pentagonal bonding face is coplanar to within 0.025(1) Å, and they are tilted at 11.48(4)° with respect to each other, slightly exposing the Ni^{IV} center between the two pairs of cage carbon atoms. The minimum distances between the nickel atom and the bonding faces of the ligands are 1.4946(2) and 1.4939(2) Å for cages *A* and *B*, respectively. This motif is typical of Ni^{IV} bis(dicarbollide) complexes but is augmented in this case, and this could be due to the steric demand of the methyl groups: the analogous angle between bonding faces in the parent metallacarborane is 5.777(8)°.[7] In contrast to the parent metallacarborane, in which the cage carbon atoms are displaced toward the nickel atom relative to the boron atoms of the bonding face, the Ni−C bond lengths in compound **1** are longer than the corresponding Ni−B bond lengths. A *cisoid* conformation is also observed in "charge-compensated" d^6 Co^{III} bis(dicarbollide) system, (*dd*/*ll*) BF$_4$[4(7),4′(7′)-(SMe$_2$)$_2$-*closo*-3,1,2-Co^{III}C$_2$B$_9$H$_{10}$-{3:3′}-*closo*-3′,1′,2′-Co^{III}C$_2$B$_9$H$_{10}$] reported by Corsini et al.,[15] in Chamberlain's Co^{III} complex, (*dd*/*ll*) [1(2),1′(2′)-(CH$_2$OCH$_2$CH$_2$OCH$_3$)$_2$-*closo*-3,1,2-Co^{III}C$_2$B$_9$H$_{10}$-{3:3′}-*closo*-3′,1′,2′-Co^{III}C$_2$B$_9$H$_{10}$],[19] and in the d^6 metal bis(*C*-monophenyldicarbollide) system, (*dd*/*ll*) Na[1(2),1′(2′)-Ph$_2$-*closo*-3,1,2-Co^{III}C$_2$B$_9$H$_{10}$-{3:3′}-*closo*-3′,1′,2′-Co^{III}C$_2$B$_9$H$_{10}$], reported by Viñas et al.[17]

Structure of (*meso*) [1,2′-Me$_2$-*closo*-3,1,2-Ni^{IV}C$_2$B$_9$H$_{10}$-{3:3′}-*closo*-3′,1′,2′-Ni^{IV}C$_2$B$_9$H$_{10}$] (2). The more soluble isomer was determined to be the *meso* diastereomer. The parent Ni^{IV} carborane, [*closo*-3,1,2-Ni^{IV}C$_2$B$_9$H$_{11}$-{3:3′}-*closo*-3′,1′,2′-Ni^{IV}C$_2$B$_9$H$_{11}$], exists as a racemate in the solid state,[7] yet has simple ^{11}B, ^{13}C, and ^{1}H NMR spectra because of a rapid contrarotation of the {C$_2$B$_9$H$_{11}$} units that interconverts racemic rotational isomers in solution.[8] As mentioned above, computational work has shown that interconversion of the rotomers may occur via two routes with similar energy barriers: through a *cisoid* conformation in which the cage carbon atoms are eclipsed, or through a conformation in which the ligands are *transoid*. In the case of compound **2**, the eclipsed conformation, where a mirror plane relates the two ligands, can only exist under the unlikely circumstance of the methyl groups occupying the same space. This may inhibit fast equilibration between the rotomers via this route, which would have to occur through this mirror plane. We also suggest that, in contrast to the nonmethylated parent species, the energy barrier to rotation through a *transoid* conformation is sufficiently high at room temperature to prevent the interconversion of rotomers. The Ni^{IV} *meso* diastereomer **2** remains asymmetric in solution at room temperature, as evidenced by the complexity of the NMR spectra (Figure 4). Two sharp and distinct methyl proton resonances at δ 1.42 and 1.74 ppm and two broader cage C−H signals at 3.06 and 3.32 ppm are observed in the 500 MHz ^{1}H NMR spectrum recorded for a toluene-d_8 solution at room temperature. At higher temperatures, however, peak coalescence occurs: the results of the variable temperature NMR experiments are discussed below. The ^{11}B NMR spectrum is similarly complicated with many signals and coincidental overlap, whereas fast interconversion of racemic rotational isomers would lead to a simplified nine-peak ^{11}B NMR spectrum, which is observed at higher temperatures.

The solid-state structure of compound **2** is represented in Figure 5. Compound **2** crystallizes as a racemate in the monoclinic space group *C*2/*c*. Crystallographically

Table 2. Selected Interatomic Distances, Angles and Torsions for Compounds **1**, **2**, $NMe_4 \cdot 3$, $MeNC_5H_5 \cdot 3$, $NMe_4 \cdot 4$, and **5**[a]

	compound						
	Ni^{IV} (**5**)	**1**	**2**	Ni^{III} (**6**)	$NMe_4 \cdot 3$	$MeNC_5H_5 \cdot 3$	$NMe_4 \cdot 4$
Ni−F*A*	1.4740(3)	1.4939(7)	1.505(1)	1.561(1)	1.587(1)	1.590(1)	1.586(1)
Ni−F*B*	1.4742(3)	1.4937(7)	1.505(1)	1.561(1)	1.587(1)	1.590(1)	1.586(1)
B10*A*···B10*B*	7.775(3)	7.831(2)	7.833(5)	7.974(6)	8.062(5)	8.066(5)	8.061(5)
F*A* ∠ F*B*	5.777(8)	11.42(6)	15.2(1)	0.0	0.0	0.0	0.0
B8*A*−*cent*(F*A*)−*cent*(F*B*)−B8*B*	35.56(2)	32.26(8)	40.5(1)	180	108.1(2)	108.0(1)	180
Ni−C1*A*	2.0773(9)	**2.134(1)**	**2.164(2)**	**2.152(1)**	**2.282(2)**	**2.284(2)**	**2.268(2)**
Ni−C2*A*	2.0649(7)	2.104(1)	2.106(2)*	2.152(1)	2.141(2)*	2.136(2)*	2.135(2)
Ni−B4*A*	2.1048(8)	2.094(1)	2.106(2)*	2.118(2)	2.130(2)*	2.144(2)*	2.144(2)
Ni−B7*A*	2.0865(4)	2.107(2)	2.094(2)	2.118(2)	2.125(2)	2.129(2)	2.090(2)
Ni−B8*A*	2.1204(5)	2.109(1)	2.099(2)	2.153(2)	2.120(2)	2.132(2)	2.156(2)
Ni−C1*B*	2.0717(4)	**2.134(1)**	2.106(2)*	2.152(1)	**2.283(2)**	**2.284(2)**	2.135(2)
Ni−C2*B*	2.0710(4)	2.093(1)	**2.164(2)**	2.152(1)	2.141(2)*	2.136(2)*	2.268(2)
Ni−B4*B*	2.1044(8)	2.096(1)	2.099(2)	2.118(2)	2.130(2)*	2.144(2)*	2.090(2)
Ni−B7*B*	2.0848(8)	2.103(1)	2.106(2)*	2.118(2)	2.125(2)	2.129(2)	2.144(2)
Ni−B8*B*	2.1151(9)	2.121(1)	2.094(2)	2.153(2)	2.120(2)	2.132(2)	2.156(2)
C1*A*−C2*A*	1.6008(5)	1.616(2)	1.660(3)§	1.588(3)	1.639(4)§	1.646(3)§	1.572(3)
C1*B*−C2*B*	1.610(1)	1.619(2)	1.660(3)§	1.588(3)	1.639(4)§	1.646(3)§	1.572(3)

[a] Data for $[Ni^{IV}(C_2B_9H_{11})_2]$ (**5**) [7] and $NMe_4[Ni^{III}(C_2B_9H_{11})_2]$ (**6**) [8] are included for comparison. Values in **bold** represent cage carbon atoms bonded to methyl groups. *These positions have partial B/C occupancy. § These bond lengths are the average of two bond lengths because of partial B/C occupancy at the 2- and 4-positions.

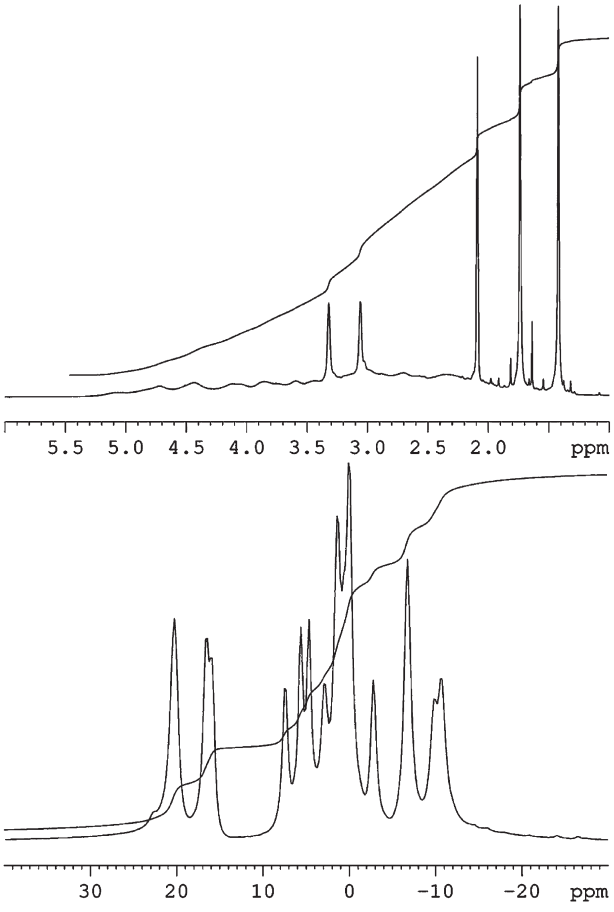

Figure 4. ^1H NMR (top) and ^{11}B-{^1H} NMR (bottom) spectra of compound **2**, recorded in toluene-d_8. The residual solvent signal appears at δ (^1H) 2.09 ppm in the ^1H NMR spectrum.

obtained dimensions are summarized in Table 2. A staggered *cisoid* conformation is observed in which the two methyl groups are in very close proximity. Because of partial B/C occupancy at the 2- and 4-positions of each cage, the molecule has a crystallographic 2-fold symmetry

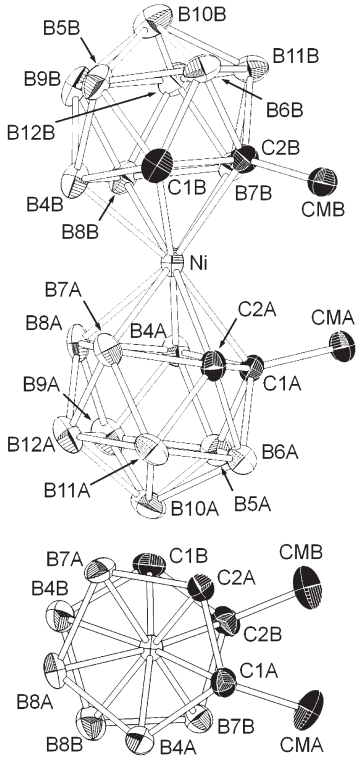

Figure 5. ORTEP representation of a single enantiomer of compound **2** with numbering scheme. Thermal ellipsoids are drawn at 50% probability, and hydrogen atoms are removed for clarity.

axis. The pentagonal bonding faces are coplanar to within 0.011(3) Å and the B8*A*−*cent*(F*A*)−*cent*(F*B*)−B8*B* torsion angle is 40.5(1)°, larger than the ideal *cisoid* angle. The tilt-angle between the bonding faces of the dicarbollide ligands of 15.28(7)°, compared to 5.777(8)° for the non-methylated parent, could be due to a possible steric interaction between the methyl groups. This crowding may also be responsible for the slightly larger Ni−F*A* and Ni−F*B* distances of 1.5059(0) Å, again compared to the non-methylated parent.

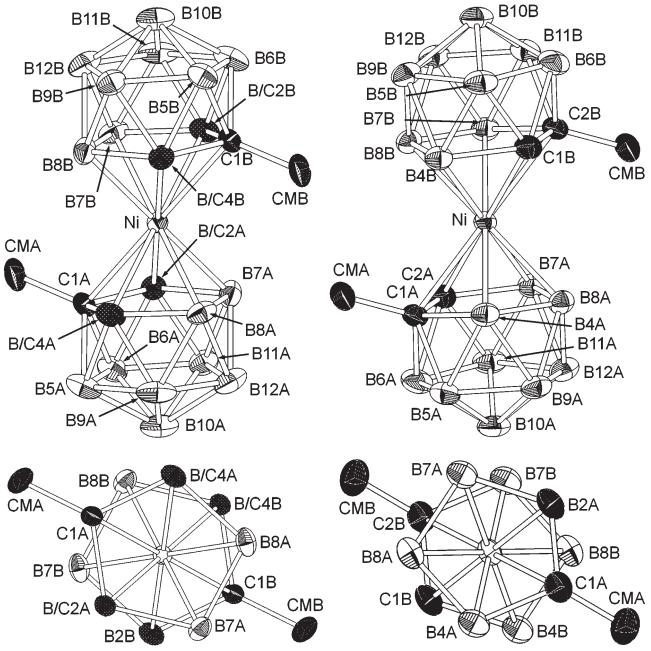

Figure 6. ORTEP representations of compounds $\mathbf{NMe_4 \cdot 3}$ (left) and $\mathbf{NMe_4 \cdot 4}$ (right) with numbering schemes, and thermal ellipsoids drawn at 50% probability. NMe_4^+ cations and hydrogen atoms are removed for clarity.

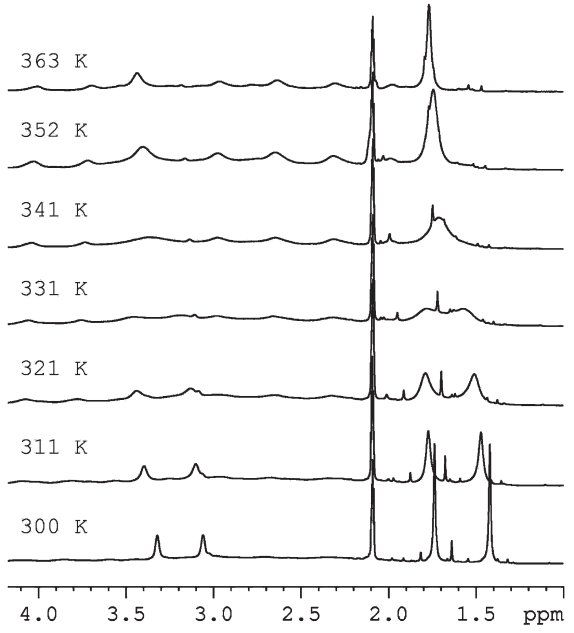

Figure 7. ^{1}H NMR spectra for compound **2** recorded in toluene-d_8 solution at various temperatures. The coalescence is reversible, and the 300 K spectrum is regenerated upon cooling the sample. Residual solvent signal appears at δ (^{1}H) about 2.09 ppm.

This result contrasts with Corsini's analogous diastereomeric "charge-compensated" d^6 Co^{III} system, (*meso*) BF_4[4,7′-$(SMe_2)_2$-*closo*-3,1,2-$Co^{III}C_2B_9H_{10}$-{3:3′}-*closo*-3′,1′,2′-$Co^{III}C_2B_9H_{10}$], where a crowded *cisoid* orientation of the SMe_2 groups is avoided through the *gauche* orientation of the dicarbollide cages.[15]

Structures of (*dd*/*ll*) $\mathbf{NMe_4}$[1(2),1′(2′)-$\mathbf{Me_2}$-*closo*-3,1,2-$\mathbf{Ni^{III}C_2B_9H_{10}}$-{3:3′}-*closo*-3′,1′,2′-$\mathbf{Ni^{III}C_2B_9H_{10}}$] ($\mathbf{NMe_4 \cdot 3}$), (*dd*/*ll*) *N*-methylpyridinium[1(2),1′(2′)-$\mathbf{Me_2}$-*closo*-3,1,2-$\mathbf{Ni^{III}}$-$\mathbf{C_2B_9H_{10}}$-{3:3′}-*closo*-3′,1′,2′-$\mathbf{Ni^{III}C_2B_9H_{10}}$] ($\mathbf{MeNC_5H_5 \cdot 3}$), and (meso) NMe_4[1,2′-Me_2-closo-3,1,2-$Ni^{III}C_2B_9H_{10}$-{3:3′}-closo-3′,1′,2′-$Ni^{III}C_2B_9H_{10}$] ($NMe_4 \cdot 4$). The purified Ni^{IV} diastereomers could be conveniently reduced to the corresponding Ni^{III} species using sodium borohydride in methanol, and precipitated from aqueous solution as a variety of salts. A single-crystal X-ray diffraction analysis was possible in each case. Salient crystallographically obtained dimensions are in Table 2, and the structures of $\mathbf{NMe_4 \cdot 3}$ and $\mathbf{NMe_4 \cdot 4}$ are represented in Figure 6.

Compound $\mathbf{NMe_4 \cdot 3}$ crystallizes in the monoclinic space group $C2/c$. The methyl groups are in a *transoid* configuration, requiring the two dicarbollide ligands to be in a *gauche* conformation. The anion is crystallographically centrosymmetric, because the second carbon atom of each dicarbollide ligand is disordered over the 2- or 4-positions, with equal occupancy of each. Because of this centrosymmetry, the bonding faces are parallel. The observed *gauche* conformation (the torsion angle, B8*A*−*cent*(F*A*)−*cent*(F*B*)−B8*B*, is 108.1(2)°) is possibly affected significantly by crystal-packing forces, and is typical of Ni^{III} bis(dicarbollide) complexes, which show no strong tendency to exhibit any particular conformation.[10,11] To confirm the structure of anion **3**, single crystals were grown with the *N*-methylpyridinium cation. Single-crystal X-ray diffraction analysis thence showed that the complex anions of compounds $\mathbf{MeNC_5H_5 \cdot 3}$ and $\mathbf{NMe_4 \cdot 3}$ are essentially isostructural. For comparison, and to confirm previously reported findings[9], single-crystal X-ray diffraction analysis was performed on the non-methylated parent anion, $NMe_4[Ni^{III}(C_2B_9H_{11})_2]$, which was synthesized following a known procedure. The crystallographically obtained dimensions for $\mathbf{MeNC_5H_5 \cdot 3}$, $\mathbf{NMe_4 \cdot 3}$, $\mathbf{NMe_4 \cdot 4}$, and $NMe_4[Ni^{III}(C_2B_9H_{11})_2]$ are presented in Table 2.

Compound $\mathbf{NMe_4 \cdot 4}$ crystallizes in the space group $C2/c$. The anion of compound $\mathbf{NMe_4 \cdot 4}$ is achiral and has a center of inversion on the nickel atom. The parallel ligand bonding-faces are coplanar to within 0.049(3)°, and the ligands are in a staggered *transoid* orientation, with *transoid* methyl groups.

Dynamics and Rotary Motion. The dynamic behavior of compounds **1** and **2** was probed with variable temperature NMR spectroscopy. The ^{11}B and ^{1}H spectra of compound **1** were measured between 168 and 300 K in a chloroform-*d*-dichloromethane-d_2 mixture, and the ^{11}B NMR spectra were measured between 300 and 410 K in xylene. At low temperatures, slight signal broadening was observed in the ^{11}B NMR, whereas raising the temperature from 273 to 410 K resulted in a slight sharpening of the ^{11}B resonance signals. This is probably due to the tumbling rate of the molecules. No information about the relative rotation of the dicarbollide ligands could be obtained from the spectra.

As mentioned above, the room-temperature ^{11}B and ^{1}H NMR spectra of compound **2** indicate that the molecule is asymmetric, with no appreciably fast interconversion of the two racemic rotational isomers. In toluene-d_8 solution, reversible coalescence of the methyl proton signals is observed in the 500 MHz ^{1}H NMR spectrum at between 335 and 340 K, indicating a barrier to interconversion of 66.5 ± 2 kJ/mol (15.9 kcal/mol) (Figure 7). This is not necessarily the barrier to a complete 360° rotation, as the

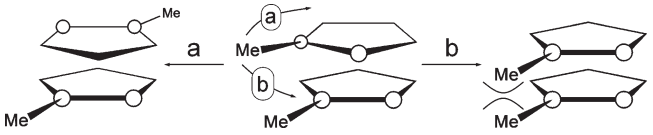

Figure 8. Interconversion of racemic rotational isomers in compound **2** may occur through an eclipsed *cisoid* (mirror plane) conformation (route *b*) or *transoid* (inversion symmetry) conformation (route *a*).

interconversion of racemic rotational isomers could occur in an oscillatory fashion through a *transoid* configuration (inversion symmetry) or an eclipsed *cisoid* configuration (mirror plane) (Figure 8). On the basis of previous calculations on the parent non-methylated nickel carborane, the highest energy barrier (about 30 kJ/mol[5] and 27.7 kJ/mol[8]) corresponds to the eclipsed *cisoid* configuration. However, the energy required for interconversion through a *transoid* configuration is very similar (about 25 kJ/mol[5] and 24.1 kJ/mol[8]). In the case of compound **2**, it is reasonable to suggest that a *cisoid* conformation, with eclipsing methyl groups, would be at very high energy, impeding interconversion by this route. We suggest that the experimentally observed 66.5 kJ/mol barrier is associated with rotation through a transoid configuration, and that this barrier is about 35 kJ/mol higher than in the parent nickel carborane because of methyl substitution. These results are comparable to those obtained by Núñez et al. in their study of the "charge-compensated" d^6 Co^{III} system, [8,8′-$(SMe_2)_2$-*closo*-3,1,2-$Co^{III}C_2B_9H_{10}$-{3:3′}-*closo*-3′1′2′-$Co^{III}C_2B_9H_{10}$].[12] They obtained, both experimentally and by calculation, rotational energy barriers of 48.1 and 49.4 kJ/mol, respectively. Clear coalescence is not observed in the ^{11}B NMR spectra. However, the onset of simplification of the ^{11}B NMR spectra occurs at 335 K, and at 363 K there are only 9 peaks with roughly equal integrals. Above about 360 K, irreversible isomerization or decomposition occurs, as evidenced by the appearance of new peaks in the ^{1}H NMR spectrum. These new peaks persist when the sample is returned to room temperature.

In the solid state, the staggered *transoid* Ni^{III} *meso* diastereomer **4** is achiral, with an inversion center on the nickel atom (Figure 1, bottom right). Upon oxidation, rotation can occur in either direction with equal probability to produce a racemic mixture of *cisoid* Ni^{IV} *meso* diastereomers **2** (Figure 1, bottom left). Reduction of a single "enantiomer" of the Ni^{IV} *meso* diastereomer would result in the loss of chirality as the complex adopts the *transoid* orientation. In the case of the *dd*/*ll* diastereomer, each staggered *gauche*-oriented Ni^{III} enantiomer **3** (Figure 1, top right) can only form the corresponding *cisoid* Ni^{IV} complex **1** (Figure 1, top left) upon oxidation through a unidirectional rotation of one-fifth of a revolution. For rotation to occur in the other direction, the methyl groups would need to pass each other, resulting in high-energy distortions of the molecule. Although it is not directly observed, the unidirectional nature of the rotation in each enantiomer may be deduced from the start and end points apparent in the solid state. It must be stressed, however, that the solid state must be compared with the solution phase with caution, as the lower-energy initial stages of the contrarotation away from the minimum-energy configuration of up to one or two tens of kJ/mol could in principle be induced by crystal-packing forces.

Conclusions

In this study, two diastereomeric pairs of nickel bis(*C*-monomethyldicarbollide) complexes, derived from the racemic [*nido*-7-CH_3-7,8-$C_2B_9H_{11}$]$^-$ anion were synthesized and characterized by NMR spectroscopy and single-crystal X-ray diffraction analysis. The presence of methyl substituents instead of hydrogen on the cage carbon atoms does not prevent the Ni^{IV} system from adopting the necessary *cisoid* configuration required for the rotor to work. In the Ni^{IV} *meso* system **2**, it has been shown that the barrier to rotation through a *transoid* configuration is sufficiently high to prevent the interconversion of racemic rotational isomers at room temperature. It is reasonable to suggest that this barrier may also exist in the *dd*/*ll* system. This is also a requirement of a useful rotor. Further chemistry is being conducted to explore the further functionalization of the dicarbollide cage to incorporate this novel rotary motion into nanoscale devices.

Acknowledgment. We gratefully acknowledge the support of this research by the National Science Foundation (NSF) (CHE-0702774 and CHE-9974928). We also thank Satish S. Jalisatgi and Alexander Safronov for assistance.

Supporting Information Available: Crystallographic experimental and summary table of crystallographic data collection and structure refinement parameters for compounds **1**, **2**, $NMe_4 \cdot$**3**, $MeNC_5H_5 \cdot$**3**, $NMe_4 \cdot$**4**, and $Me_4N[Ni^{III}(C_2B_9H_{11})_2]$ (Table S1), CIF files for these structures, and comparisons of crystallographic and conventional carborane numbering schemes. This material is available free of charge via the Internet at http://pubs.acs.org.